THE JOURNAL OF BIOLOGICAL CHEMISTRY VOL. 289, NO. 49, pp. 33754–33766, December 5, 2014

Identification and Functional Characterization of the Phosphorylation Sites of the Neuropeptide FF_2 Receptor*

Received for publication, September 17, 2014, and in revised form, October 10, 2014 Published, JBC Papers in Press, October 17, 2014, DOI 10.1074/jbc.M114.612614

Lauriane Bray, Carine Froment, Pierre Pardo, Cédric Candotto, Odile Burlet-Schiltz, Jean-Marie Zajac, Catherine Mollereau[1,2], and Lionel Moulédous[1,3]

From the Institut de Pharmacologie et Biologie Structurale, UMR5089 CNRS, Université de Toulouse, 31077 Toulouse, France

Background: G protein-coupled receptor functions are regulated by phosphorylation.
Results: Mass spectrometry was used to map the phosphorylation sites of the $NPFF_2$ neuropeptide FF receptor, and site-directed mutagenesis permitted the identification of their role in receptor regulation.
Conclusion: Sites involved in desensitization and internalization do not fully overlap.
Significance: This is the first mapping of $NPFF_2$ receptor phosphorylation.

The neuropeptide FF_2 ($NPFF_2$) receptor belongs to the rhodopsin family of G protein-coupled receptors and mediates the effects of several related RFamide neuropeptides. One of the main pharmacological interests of this system resides in its ability to regulate endogenous opioid systems, making it a potential target to reduce the negative effects of chronic opioid use. Phosphorylation of intracellular residues is the most extensively studied post-translational modification regulating G protein-coupled receptor activity. However, until now, no information concerning $NPFF_2$ receptor phosphorylation is available. In this study, we combined mass spectrometric analysis and site-directed mutagenesis to analyze for the first time the phosphorylation pattern of the $NPFF_2$ receptor and the role of the various phosphorylation sites in receptor signaling, desensitization, and trafficking in a SH-SY5Y model cell line. We identified the major, likely GRK-dependent, phosphorylation cluster responsible for acute desensitization, ^{412}TNST^{415} at the end of the C terminus of the receptor, and additional sites involved in desensitization (^{372}TS^{373}) and internalization (Ser^{395}). We thus demonstrate the key role played by phosphorylation in the regulation of $NPFF_2$ receptor activity and trafficking. Our data also provide additional evidence supporting the concept that desensitization and internalization are partially independent processes relying on distinct phosphorylation patterns.

Neuropeptide FF_2 ($NPFF_2$)[4] receptor belongs to the rhodopsin family of G protein-coupled receptors (GPCR) (1, 2). It mediates the effects of several RFamide neuropeptides produced from two precursors called proNPFF$_A$ and proNPFF$_B$ (3). The NPFF system is involved in a variety of physiological processes affecting cardiovascular function and pain perception, among other processes (4). One of its main pharmacological interests resides in its ability to regulate endogenous opioid systems, making it a potential target to reduce the negative effects of chronic opioid use (5–7). Indeed, the NPFF receptor antagonist RF9 has been shown to prevent the development of tolerance and hyperalgesia induced by chronic heroin treatment in rats (8), as well as morphine tolerance and physical dependence in mice (9). The signaling properties of the $NPFF_2$ receptor have been studied in several cellular models. The receptor was demonstrated to couple to $G_{i/o}$ heterotrimeric proteins to inhibit adenylyl cyclase (10) and N-type voltage-gated calcium channels (11) and activate G protein-regulated inwardly rectifying potassium channels (12), as well as a putative delayed rectifier K^+ channel (13). It was also shown to activate MAPK pathways (14). However, the mechanisms regulating $NPFF_2$ receptor signaling and trafficking have not been studied in detail.

Phosphorylation of intracellular residues is the most extensively studied post-translational modification regulating GPCR activity. After agonist binding, homologous phosphorylation of activated GPCR, mediated by kinases belonging to the GPCR kinase family (GRK), results in G protein uncoupling, the first step of receptor desensitization (15, 16). Recent evidence suggests that GRK could also be involved in heterologous phosphorylation (meaning, upon activation of another GPCR) and desensitization (17, 18). Second messenger-dependent kinases such as PKA or PKC can also promote desensitization (15, 16). Phosphorylation of activated receptors then triggers the recruitment of β-arrestin1 and/or arrestin2 proteins (also called arrestin2 and arrestin3, respectively) (19), which contributes to G protein uncoupling and clathrin-coated pit-mediated receptor internalization but can also elicit G protein-independent signaling (20). In recent years, it has appeared that phosphorylation was not a simple on/off switch for GPCR activity but that, depending on ligand or cell type, various patterns of receptor phosphorylation, sometimes referred to as barcoding, could regulate receptor function in different ways (21–24).

* This work was supported in part by grants from the Fondation pour la Recherche Médicale (programme Grands Equipements), the Région Midi-Pyrénées, Infrastructures en Biologie, Santé et Agronomie, and Fonds Européens de Développement Régional.
[1] These authors contributed equally to this work.
[2] To whom correspondence may be addressed: Inst. de Pharmacologie et Biologie Structurale, UMR5089 CNRS, Université de Toulouse, 205 route de Narbonne BP64182, 31077 Toulouse, France. E-mail: catherine.mollereau-manaute@ipbs.fr.
[3] To whom correspondence may be addressed: Inst. de Pharmacologie et Biologie Structurale, UMR5089 CNRS, Université de Toulouse, 205 route de Narbonne BP64182, 31077 Toulouse, France. E-mail: Lionel.mouledous@ipbs.fr.
[4] The abbreviations used are: $NPFF_2$, neuropeptide FF_2; GPCR, G protein-coupled receptor; GRK, GPCR kinase; PTX, pertussis toxin; KRH, Krebs-Ringer-HEPES; CID, collision-induced dissociation; ETD, electron transfer dissociation.

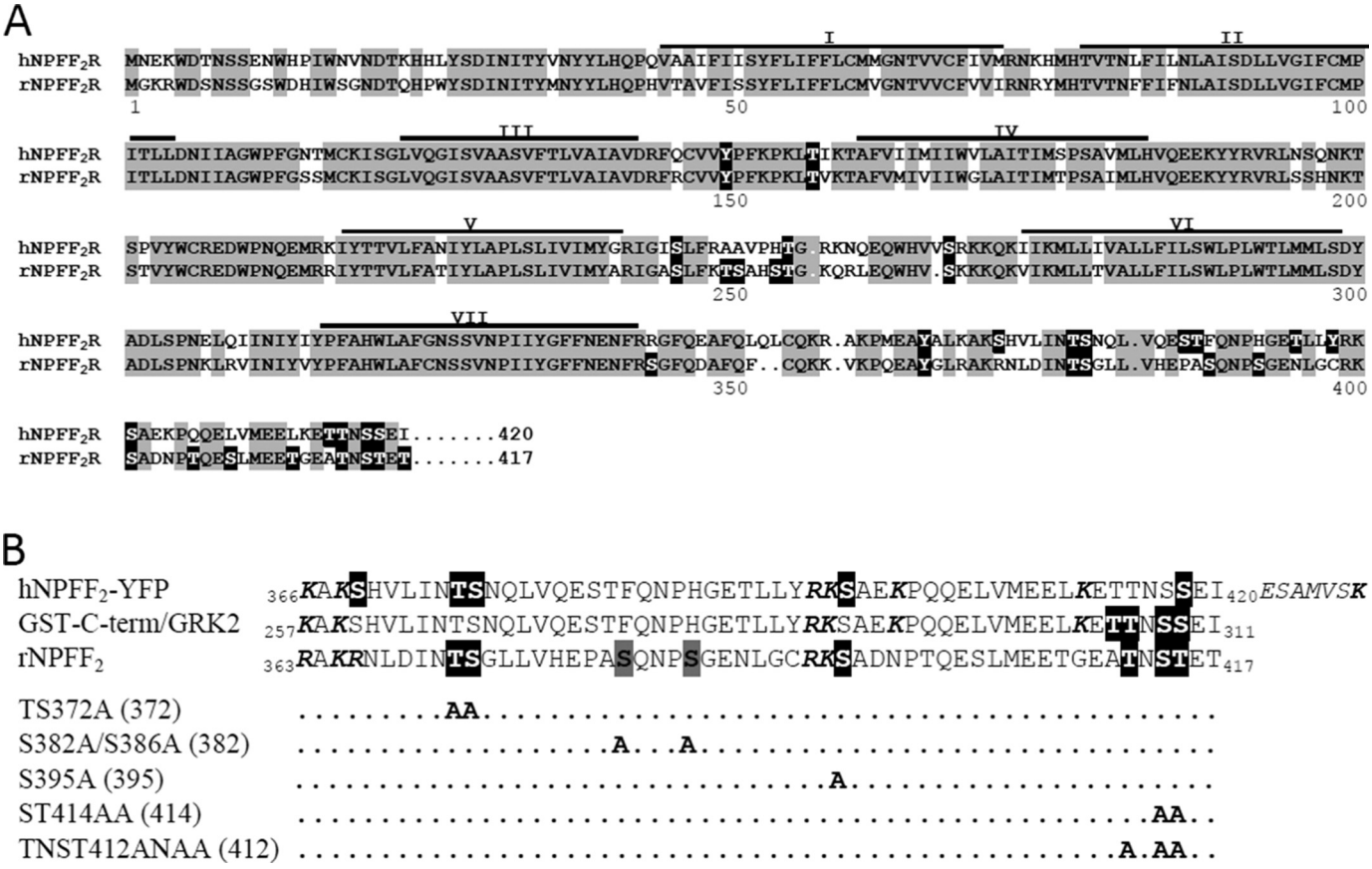

FIGURE 1. **Sequence alignments of human and rat NPFF$_2$ receptors.** *A*, full sequences. *Gray shading* indicates sequence similarity between species. *Black shading* shows all the putative phosphorylation sites. *B*, alignment of the C-terminal NPFF$_2$ receptor sequences found to be phosphorylated in SH-SY5Y cells expressing hNPFF$_2$-YFP or T7-rNPFF$_2$ receptors or to be *in vitro* phosphorylated by GRK2 within the GST-thrombine-hNPFF$_2$ C-terminus construct. *Black shading* indicates the phosphorylated sites unambiguously identified by nanoLC-MS/MS except for those specific to rat, which are highlighted with *gray shading*. *Bold italic characters* show the trypsin cleavage sites. *Small italic capitals* correspond to the sequence of the linker plus the first YFP residues fused to the hNPFF$_2$ receptor C terminus. The positions of alanine substitutions in the different T7-rNPFF$_2$ mutant receptors are presented. The simplified name of each mutant is in *brackets*.

From a fundamental point of view, it is thus important to map the phosphorylation pattern of GPCR and to characterize the specific contribution of each phosphorylated site to the regulation of receptor activity (25, 26). Agonist-dependent phosphorylation sites can also be targeted to generate phospho-specific antibodies useful to study receptor activation *in vivo* (27). In the case of rodent NPFF receptors such tools are lacking and could be very helpful for understanding physiological activation of these receptors. However, to date, the potential phosphorylation sites of NPFF$_2$ receptors have never been studied. Depending on the species, 20 or more Ser, Thr, or Tyr candidates are present in the intracellular domain of the receptor (Fig. 1). Because of this potential complexity, we first undertook a mass spectrometry approach to map phosphorylated residues in the human and rat NPFF$_2$ receptors in a SH-SY5Y neuroblastoma cellular model (18). Site-directed mutagenesis was then performed to study the role of phosphorylated residues/clusters in receptor signaling, desensitization, and trafficking.

EXPERIMENTAL PROCEDURES

Materials—Oligonucleotides were synthesized by Sigma Genosys. Restriction enzymes were purchased from New England Biolabs (Ozyme, France). Anti-T7 monoclonal antibody was from Merck Millipore. Rabbit anti-p44/42 MAPK and anti-phospho(Thr^{202}/Tyr^{204})-p44/42 MAPK antibodies were from Cell Signaling Technology (Ozyme, France). Alexa Fluo 488 goat anti-mouse, rabbit anti-phosphothreonine and monoclonal mouse anti-GFP (mAb3E6) antibodies were from Invitrogen. HRP-coupled goat anti-rabbit IgG and anti-mouse IgG were purchased from Jackson ImmunoResearch. 1DMe ([D-Tyr^1, (NMe)Phe^3]NPFF) (28) was synthesized with an automated peptide synthesizer (model 433A; Applied Biosystems). Pertussis toxin (PTX) and chelerythrin were from Sigma. PLC inhibitor (U73122), calmodulin inhibitor (W7), and β-ARK1 inhibitor were from Calbiochem (Merck Millipore). [^{3}H]adenine (26 Ci/mmol) was purchased from GE Healthcare. The NPFF$_2$ receptor-selective radioligand [^{3}H]EYF (Glu-Tyr-Trp-Ser-Leu-Ala-Ala-Pro-Gln-Arg-Phe-NH$_2$) was tritiated by Tritec (Switzerland) as described (29). All other reagents were from Sigma or Euromedex (France).

Vector Construction and Site-directed Mutagenesis—T7-rNPPF$_2$ receptor: PCR was used to amplify a cDNA coding the rat NPFF$_2$ receptor from a pCDN vector (generous gift from Dr. S. Krief). PCR primers were designed to introduce an AfeI restriction site at the 5′ end (catataagcgctatgggcaagagatgggactcaaactct) and a stop codon and a XbaI site at the 3′ end (aatcctctagactaagtctcagtactgttggtagcttctccc) of the amplified fragment. The

fragment was then cloned in frame with a T7 peptide tag in pRc/CMV vector. Phosphosites/alanine exchange: site-directed mutations were introduced in the T7-rNPPF$_2$ sequence by PCR using the QuikChange Lightning site-directed mutagenesis kit (Stratagene, Agilent Technologies Company, France) according to the manufacturer's instructions. The following primers were used: TS372AA (sense, acgcaacctggacataaacgcagctggcctgttggtc; antisense, gaccaacaggccagctgcgtttatgtccaggttgcgt), S382A/S386A (sense, gtccatgaacctgcagctcaaaacccagctggggaaaacttgg; antisense, ccaagttttccccagctgggttttgagctgcaggttcatggac), S395A (sense, tggggaaaacttgggatgtagaaaagctgcagacaatccc; antisense, gggattgtctgcagcttttctacatcccaagttttccccca), ST414AA (sense, aaacgggagaagctaccaacgctgctgagacttagtctagaggg; antisense, ccctctagactaagtctcagcagcgttggtagcttctcccgttt), and TNST412ANAA (sense, aaacgggagaagctgccaacgctgcagagacttagtctag; antisense, ctagactaagtctctgcagcgttggcagcttctccccgttt). For the GST-hNPFF$_2$ C terminus construct, PCR was used to amplify a cDNA coding the last 85 amino acids of the C terminus of the human NPFF$_2$ receptor. PCR primers were designed to introduce a BamHI restriction site at the 5′ end (cgcggatccttcaacgagaacttc) and a stop codon and an EcoRI site at the 3′ end (ggaattcttaaatctcactgctgttag) of the amplified fragment. The fragment was then cloned in frame with GST followed by a thrombin cleavage site in the pGEX2T vector (GE Healthcare). All constructs were verified by sequencing (Millegen, Toulouse, France).

Cell Culture and Transfection—Human neuroblastoma SH-SY5Y cells were grown in Dulbecco's modified Eagle's medium (4.5 g/liter glucose, GlutaMAX) containing 10% FCS and 50 μg/ml gentamicin (all from Invitrogen), in a 37 °C humidified atmosphere containing 5% CO_2. All stable cDNA transfections were performed according to the manufacturer's instruction using FuGENE 6 (Roche Diagnostics). After transfection of WT or mutant T7-rNPFF$_2$ receptors, 500 μg/ml G418 (Invitrogen) was added to the culture medium for selection of clones. For SH-SY5Y cells transfected with hNPFF$_2$-YFP receptor (30), 5 μg/ml blasticidin (Cayla, Invivogen, France) was added to the culture medium. All cells were used undifferentiated.

Binding and cAMP Measurement Assays—SH-SY5Y cells stably expressing WT or mutant T7-rNPFF$_2$ receptors were characterized by [^{3}H]EYF binding on membrane preparations and by cellular cAMP assays, as described previously (29, 31).

Receptor Immunoprecipitation—Cells grown to 80% confluence in 140-mm culture dishes were incubated in medium containing 0.5% FCS for 2 h. After a wash in Krebs-Ringer-HEPES (KRH) buffer (124 mM NaCl, 5 mM KCl, 1.25 mM $MgSO_4$, 1.5 mM $CaCl_2$, 1.25 mM KH_2PO_4, 25 mM HEPES, 8 mM glucose, 0.5 mg/ml bovine serum albumin, pH 7.4), the cells were incubated with the agonist 1DMe (1 μM) in KRH buffer for 30 min at room temperature. They were then scraped directly on ice and centrifuged at 1000 × *g* for 10 min at 4 °C. The pellet was incubated for 1 h at 4 °C under gentle agitation in lysis buffer (50 mM Tris-HCl, pH 7.4, 150 mM NaCl, 5 mM EDTA, 0.5% Nonidet P-40) containing protease and phosphatase inhibitor mixtures (Complete EDTA-free and PhosphoStop, respectively; Roche Diagnostics). The homogenate was then centrifuged at 20,000 × *g* for 2 min at 4 °C, and the supernatant was collected. hNPFF$_2$-YFP receptors were immunoprecipitated by using monoclonal anti-GFP antibodies exactly as described in Ref. 18. T7-rNPFF$_2$ receptors were immunoprecipitated by overnight incubation at 4 °C with T7 tag agarose beads (EMD Millipore Merck) followed by three washes in 50 mM Tris-HCl, 0.5% Nonidet P-40, 5 mM EDTA. For mass spectrometry analysis, samples were resuspended in 2× Laemmli sample buffer containing 30 mM DTT, boiled for 5 min at 100 °C, and alkylated in 90 mM iodoacetamide for 30 min in the dark. For standard Western blots, samples were resuspended in 2× Laemmli sample buffer containing 5% mercaptoethanol and boiled for 5 min at 100 °C.

GST-hNPFF$_2$ C Terminus Purification and in Vitro Phosphorylation—GST fusion proteins were purified using the MicroSpin GST Purification Module (GE Healthcare) according to the manufacturer's instructions. Following induction with 0.2 mM isopropyl β-D-thiogalactopyranoside, transformed BL21 *E. coli* were lysed by sonication in a buffer containing 50 mM Tris, 2 mM EDTA, 0.1% Triton X-100, 1 mg/ml lysozyme, and protease inhibitors (Complete EDTA-free cocktail; Roche Diagnostics). After centrifugation of the lysate, the supernatant was loaded on a Microspin GST column that was washed with PBS, then with PBS with 0.1% Triton X-100, and finally with PBS with 400 mM NaCl. The protein of interest was eluted in 50 mM Tris-HCl, pH 8, containing 10 mM glutathion. The purified fragment (4 μg) was submitted to *in vitro* phosphorylation with GRK2 (0.4 μg, a generous gift from Prof. J. Benovic, Thomas Jefferson University, Philadelphia, PA) in a buffer containing 20 mM HEPES, 1 mM DTT, 1 mM EDTA, 5 mM $MgCl_2$, and 200 μM ATP for 2h at 30 °C in a final volume of 20 μl. The sample was then prepared for proteomic analysis as described above.

In-gel Tryptic Digestion and NanoLC-MS/MS Analysis—Proteins were separated by SDS-PAGE on 10% polyacrylamide gels. Gels were stained with colloidal Coomassie Blue (17% (w/v) ammonium sulfate, 34% (v/v) methanol, 3% (v/v) orthophosphoric acid, and 0.1% (w/v) Brilliant Blue G-250) for 24 h. Bands corresponding to T7-rNPFF$_2$ (95 kDa) receptor, hNPFF$_2$-YFP receptor (130 kDa) or GST-hNPFF$_2$ C terminus (36 kDa) were excised and subjected to in-gel tryptic digestion as described previously (18). The hNPFF$_2$-YFP and T7-rNPFF$_2$ dried peptide extracts obtained were then analyzed by on-line nanoLC using an Ultimate 3000 System (Dionex, Amsterdam, The Netherlands) coupled to an electron transfer dissociation (ETD)-enabled LTQ Orbitrap Velos mass spectrometer (Thermo Fisher Scientific) for an alternative decision tree-driven collision-induced dissociation (CID)/ETD fragmentation acquisition (27). For GST-Thrombin-hNPFF$_2$ C terminus dried peptide extracts, online nanoLC-MS/MS analyses were performed using an Ultimate 3000 system (Dionex) coupled to an nanospray LTQ Orbitrap XL mass spectrometer (Thermo Fisher Scientific). The LTQ Orbitrap XL was operated in data-dependent acquisition mode with the XCalibur software (version 2.0 SR2; Thermo Fisher Scientific), using a 60-s dynamic exclusion window to prevent repetitive selection of the same peptide. The survey scan MS was performed in the Orbitrap on the 300–2000 m/z mass range with the resolution set to a value of 60,000 at m/z 400. The five most intense ions per survey scan were selected for MS/MS fragmentation, and the resulting frag-

ments were analyzed in the linear trap (parallel mode). The normalized collision energy was set to 35%.

Database Search and Determination of NPFF$_2$ Receptor Phosphopeptide Abundance Ratio—Peak lists extraction from Xcalibur raw files were automatically performed using Proteome Discoverer software (version 1.4, Thermo Fisher Scientific, France). Parameters were set as previously described (18) with the following modifications. Peak lists were searched against SwissProt and TrEMBL human or rat databases implemented with the YFP-tagged hNPFF$_2$, T7-tagged rNPFF$_2$, or GST-Thrombin-hNPFF$_2$ C terminus sequence and using Mascot software (version 2.3.01; Matrix Science). Up to three missed trypsin cleavages were allowed. Mass tolerances in MS and MS/MS were set to 10 ppm and 0.6 Da, respectively, for hNPFF$_2$-YFP and T7-rNPFF$_2$. For GST-Thrombin-hNPFF$_2$ C terminus, mass tolerances were set to 10 ppm and 0.8 Da. The phosphorylation site localization of identified phosphopeptides was performed by phosphoRS algorithm 3.1 (32) implemented in Proteome Discoverer. A site localization probability of at least 0.75 was used as the threshold for the phosphoresidue localization. Peak areas were automatically measured from extracted ion chromatograms of each peptide (sum of all observed charge states) in the nanoLC-MS raw file using the label-free module of the in-house developed MFPaQ version 4.0.0 software (33). To calibrate the amounts of NPFF receptor in the different samples, normalization was performed based on the sum of the extracted ion chromatogram areas of identified NPFF receptor reference peptides (unmodified and unequivocally cleaved peptides, always present in all samples). The reference peptides for the hNPPF$_2$-YFP receptor were: ^{200}TSPVYWCR^{207} in the NPFF2 receptor sequence and ^{428}GEELFTGVVPILVELDGDVNGHK^{450}, ^{451}FSVSGEGEGDATYGK^{465}, ^{470}FICTTGK^{476}, ^{565}LEYNYNSHNVYIMADK^{580}, ^{593}HNIEDGSVQLADHYQQNTPIGDGPVLLPDNHYLSYQSK^{630} in the YFP sequence.

Western Blot Analysis of NPFF$_2$ Receptor and ERK Phosphorylation—Cells expressing WT or mutant T7-rNPFF$_2$ receptors were grown to 80% confluence in 100-mm culture dishes or in 24-well plate for ERK phosphorylation assay. After 2 h of incubation in medium containing 0.5% FCS, the cells were incubated in KRH buffer containing the agonist 1DMe (1 μM) for 2–30 min at room temperature. For the pharmacological inhibitor tests, PTX (100 ng/ml) was applied to the cells for 16–18 h, the βARK1 inhibitor (50 μM) was added during the 2-h incubation in deprived serum, and the PKC inhibitor chelerythrine (10 μM) and the calmodulin inhibitor W7 (20 μM) were applied together with the agonist. The cells were scraped on ice and processed for T7 immunoprecipitation as described above or directly scrubbed in Laemmli sample buffer for ERK phosphorylation assay. Proteins were separated by SDS-PAGE on 10% polyacrylamide gels and transferred to PVDF membrane for immunoblotting under standard conditions in Tris-buffered saline (20 mM Tris, pH 7.6, 137 mM NaCl) containing 0.2% Tween and 1% BSA for rabbit phosphothreonine antibody (Invitrogen; 1 μg/ml) and 5% BSA for the other primary antibodies. Immunoreactivity was revealed with peroxidase-conjugated goat anti-rabbit or anti-mouse IgG antibodies using the Pierce ECL2 Western blotting substrate (Thermo Fisher Scientific). X-ray films were scanned using a GS-800 or GS-900 calibrated densitometer (Bio-Rad). Blots were quantified using Quantity One software (Bio-Rad) with total T7-NPFF$_2$ receptor or total ERK as internal standards.

Calcium Imaging—Measurement of $[Ca^{2+}]_i$ was performed in perfused WT and mutant receptor expressing SH-SY5Y cells by quantitative photometry using the fluorescent Ca^{2+} indicator Fluo-4-AM as described previously (31).

Immunocytochemistry—Cells were seeded on glass coverslips in 24-well plates the day before the experiment. The cells were washed with KRH buffer and incubated for 30 min in KRH (control) or KRH containing 1 μM 1DMe at room temperature. The cells were then rinsed three times with ice-cold PBS, fixed, and permeabilized in ice-cold PBS containing 3.7% paraformaldehyde and 0.2% Triton X-100. After three washes, cells were incubated in PBS containing 10% FCS, 2% BSA for 1 h at room temperature, and then incubated with anti-T7 antibody (1/2000) in PBS, 2% FCS overnight at 4 °C. After three washes, cells were incubated with Alexa Fluor 488 goat anti-mouse antibodies for 1 h at room temperature in the dark. The cells were washed three more times, mounted in Vectashield medium (Vector Laboratories, AbCys, France), and observed on an Olympus (FV1000) inverted confocal microscope with a 60×/NA1.4 objective at 488-nm excitation wavelength. Images were processed with ImageJ (National Institutes of Health). Quantification of internalization was performed using Metamorph (Molecular Devices). For each cell, the average fluorescence intensity at the membrane and the average fluorescence intensity of the whole cell were measured. Then for each experiment the internalization level was calculated as follows: 100 − [((1DMe plasma membrane fluorescence/1DMe total cell fluorescence) × 100)/(control plasma membrane fluorescence/control total cell fluorescence)].

β-Arrestin2 Recruitment—Transient transfection of β-arrestin2-GFP (generous gift from Dr. S. Allouche, Université de Caen, Caen, France) was realized by using the Nucleofector technology (Lonza Cologne AG) according to the manufacturer's instructions. After electroporation, the cells were seeded on glass coverslips in 24-well plates. 48 h post-transfection, the cells were incubated in medium containing 0.5% FCS for 2 h. After a wash in KRH buffer, the cells were incubated at room temperature in the presence of the agonist 1DMe (1 μM) for 30 min and then fixed, mounted, and observed on an Olympus (FV1000) inverted confocal microscope with a 60-/NA1.4 objective.

Data Analysis—Nonlinear regressions and statistical analyses of the data were performed using Prism 5 (GraphPad Software Inc.) as described in the figure legends.

RESULTS

Mass Spectrometric Analysis of NPFF$_2$ Receptor Phosphorylation—To characterize the phosphorylation pattern of the human NPFF$_2$ receptor, we used a stable SH-SY5Y cell line expressing the receptor fused to YFP at its C terminus. The receptor was purified by GFP immunoprecipitation followed by SDS-PAGE for subsequent mass spectrometry analysis. Fig. 2*A* shows the hNPFF$_2$-YFP receptor detected with a GFP antibody after GFP immunoprecipitation (*left panel*) and a preparative

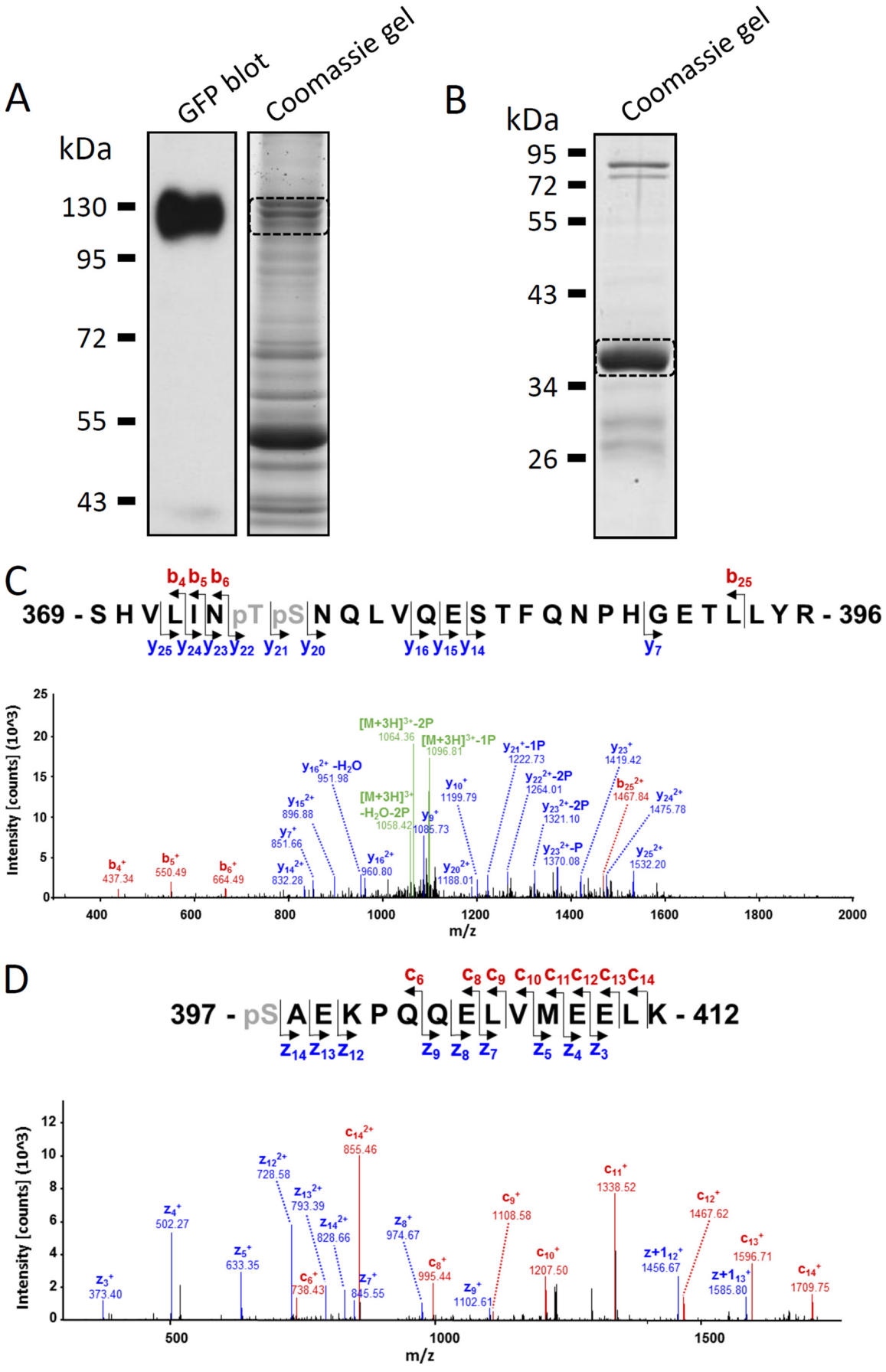
A
GFP blot
Coomassie gel
kDa
130
95
72
55
43
B
Coomassie gel
kDa
95
72
55
43
34
26
C
369 - S H V L I N pT pS N Q L V Q E S T F Q N P H G E T L L Y R - 396
b4 b5 b6
b25
y25 y24 y23 y22 y21 y20
y16 y15 y14
y7
Intensity [counts] (10^3)
m/z
[M+3H]3+-2P 1064.36
[M+3H]3+-1P 1096.81
y21+-1P 1222.73
y23+ 1419.42
y16 2+ -H2O 951.98
y10+ 1199.79
y22 2+-2P 1264.01
b25 2+ 1467.84
y24 2+ 1475.78
y15 2+ 896.88
[M+3H]3+ -H2O-2P 1058.42
y9+ 1085.73
y23 2+-2P 1321.10
y7+ 851.66
y23 2+-P 1370.08
y25 2+ 1532.20
b4+ 437.34
b5+ 550.49
b6+ 664.49
y14 2+ 832.28
y16 2+ 960.80
y20 2+ 1188.01
D
397 - pS A E K P Q Q E L V M E E L K - 412
c6
c8 c9 c10 c11 c12 c13 c14
z14 z13 z12
z9 z8 z7
z5 z4 z3
Intensity [counts] (10^3)
m/z
c14 2+ 855.46
z12 2+ 728.58
z13 2+ 793.39
c11+ 1338.52
z4+ 502.27
z14 2+ 828.66
c9+ 1108.58
c12+ 1467.62
z8+ 974.67
c13+ 1596.71
z5+ 633.35
c8+ 995.44
c10+ 1207.50
z+1 12+ 1456.67
c14+ 1709.75
z3+ 373.40
c6+ 738.43
z7+ 845.55
z9+ 1102.61
z+1 13+ 1585.80

TABLE 1

List of the phosphorylated hNPFF$_2$ receptor peptides, their unphosphorylated counterparts identified by nanoLC-MS/MS in SH-SY5Y cells, and the peptides found to be phosphorylated *in vitro* by GRK2 within the GST-thrombin-hNPFF$_2$ C terminus construct

Phosphorylation sites are in bold and underlined, with parentheses pointing out ambiguity on the position. Peptides were quantified using the label-free module implemented in the MFPaQ v4.0 software, and their amounts were calibrated in each sample, based on the NPFF receptor reference peptides described under "Experimental Procedures." The peptide ratio 1DMe/control corresponds to the ratio of the calibrated pairwise peak intensities from agonist over buffer-treated cells and are expressed as means ± S.E. (*n*) indicates how many times the peptide was identified over five experiments. In the case where a peptide identified in one condition was not identified in the other one, a value corresponding to the peak area of the peptides of the lowest abundance (5th percentile) among all the peptides identified in the sample was assigned to the missing data. *In vitro* phosphorylation data are representative of two independent experiments. MC, missed cleavage; Theo. mass, theoretical mass; Position, amino acid positions in each construct (full-length receptor fused to YFP or receptor C terminus fused to GST).

Theo. mass	MC	Positions	Sequence	Phospho-residue	Peptide ratio (1DMe/control)
hNPFF$_2$-YFP					
3423.753489	1	367–396	AKSHVLINTSNQLVQESTFQNPHGETLLYR		1.279661 (1)
3503.719818	1	367–396	AK**S**HVLINTSNQLVQESTFQNPHGETLLYR **1P**	Ser(P)^{369}	0.46591 ± 0.240 (3)
3583.686148	1	367–396	AK**S**HVLIN**(T)(S)**NQLVQESTFQNPHGETLLYR **2P**	Ser(P)^{369} and Thr(P)^{375} or Ser(P)^{376}	65.4386 (1)
3224.621415	0	369–396	SHVLINTSNQLVQESTFQNPHGETLLYR		0.57760 ± 0.232 (5)
3304.587744	0	369–396	SHVLIN**(T)(S)**NQLVQESTFQNPHGETLLYR **1P**	Thr(P)^{375} or Ser(P)^{376}	6.23368 ± 3.291 (3)
3304.587744	0	369–396	SHVLINT**S**NQLVQESTFQNPHGETLLYR **1P**	Ser(P)^{376}	13.4880 ± 5.246 (2)
3384.554074	0	369–396	SHVLIN**TS**NQLVQESTFQNPHGETLLYR **2P**	Thr(P)^{375} and Ser(P)^{376}	10.43478 (1)
3384.554074	0	369–396	**S**HVLINT**S**NQLVQESTFQNPHGETLLYR **2P**	Ser(P)^{369} and Ser(P)^{376}	32.2807 (1)
1757.886929	1	398–412	SAEKPQQELVMEELK		0.59079 ± 0.123 (5)
1837.853258	1	398–412	**S**AEKPQQELVMEELK **1P**	Ser(P)^{398}	0.52069 ± 0.165 (5)
1885.981889	2	397–412	KSAEKPQQELVMEELK		0.38205 ± 0.050 (5)
1965.9482	2	397–412	K**S**AEKPQQELVMEELK **1P**	Ser(P)^{398}	0.28522 ± 0.062 (2)
3479.701103	3	397–427	KSAEKPQQELVMEELKETTNSSEI*ESAMVSK*		0.14200 ± 0.072 (5)
3559.677252	3	397–427	K**S**AEKPQQELVMEELKETTNSSEI*ESAMVSK* **1P**	Ser(P)^{398}	0.04044586 (1)
3351.606143	2	398–427	SAEKPQQELVMEELKETTNSSEI*ESAMVSK*		0.21746 ± 0.059 (5)
3431.572472	2	398–427	**S**AEKPQQELVMEELKETTNSSEI*ESAMVSK* **1P**	Ser(P)^{398}	0.13638 ± 0.071 (2)
1611.729779	0	413–427	ETTNSSEI*ESAMVSK*		0.23246 ± 0.039 (5)
1691.696108	0	413–427	ETTNS**S**EI*ESAMVSK* **1P**	Ser(P)^{418}	0.36032 ± 0.136 (3)
hNPFF$_2$ C-terminal/*in vitro* GRK2					
2827.319763	3	288–311	KSAEKPQQELVMEELKET**T**NSSEI **1P**	Thr(P)^{415}	
2827.319763	3	288–311	KSAEKPQQELVMEELKE**T**TNSSEI **1P**	Thr(P)^{414}	
2827.319763	3	288–311	KSAEKPQQELVMEELKE**T**TN**S**SEI **1P**	Ser(P)^{417}	
2907.286087	3	289–311	KSAEKPQQELVMEELKET**T**N**(S)(S)**EI **2P**	Thr(P)^{415} and Ser(P)^{417} or Ser(P)^{418}	
2699.224808	2	289–311	SAEKPQQELVMEELKET**T**NSSEI **1P**	Thr(P)^{415}	
2699.224808	2	289–311	SAEKPQQELVMEELKETTN**S**SEI **1P**	Ser(P)^{417}	
2699.224808	2	289–311	SAEKPQQELVMEELKETTNS**S**EI **1P**	Ser(P)^{418}	
2779.191132	2	289–311	SAEKPQQELVMEELKET**T**NS**S**EI **2P**	Thr(P)^{415} and Ser(P)^{418}	

Coomassie gel used to isolate the immunoprecipitated receptor for nanoLC-MS/MS analysis. Data-dependent decision tree-based CID/ETD analyses associated to phosphoRS algorithm calculation were used for more confident localization of phosphorylation sites. The peptides specific to the hNPFF$_2$-YFP receptor corresponded to 25 ± 4% of the total MS signal (n = 10). CID gave a coverage of the receptor sequence ranging from 38 to 51%, whereas ETD gave a coverage between 19 and 43%.

To characterize the agonist-induced phosphorylation of the NPFF$_2$ receptor, cells were treated with or without 1DMe, a stable NPFF analog (28) (1 μM) for 30 min at room temperature before receptor isolation and nanoLC-MS/MS analysis. The list of identified phosphorylated peptides together with their unphosphorylated counterparts is given in Table 1. Except for Thr^{157} in the second intracellular loop, all the putative phosphorylation sites (Fig. 1) were covered by the analysis. Phosphorylated residues were detected only in the last part of the receptor C terminus. Examples of spectra obtained with each dissociation mode are given in Fig. 2*C*.

The first peptide, SHVLINTSNQLVQESTFQNPHGETLLYR, was sometimes extended by two residues (AK) at its N terminus because of a missed cleavage. It was present in different forms: unphosphorylated, phosphorylated either on Ser^{369}, Thr^{375}, or Ser^{376}, or finally dually phosphorylated on a combination of those three residues. Agonist treatment increased the abundance of peptides phosphorylated on Thr^{375} and/or Ser^{376}, whereas that of unphosphorylated or Ser^{369}-phosphorylated peptides was decreased (Table 1). This indicates that basal phosphorylation of Ser^{369} is not regulated by the agonist, whereas receptor activation induces the phosphorylation of the ^{375}TS^{376} doublet.

Data concerning the last receptor fragment (fused to the first residues of YFP), KSAEKPQQELVMEELKETTNSSEI*ESAMVSK*, were more difficult to interpret. Trypsin digestion was not fully efficient, giving rise to peptides of various sizes with up to three missed cleavages (Table 1). Among these peptides, only two phosphorylation sites could be reproducibly identified: Ser^{398} and Ser^{418}. Unexpectedly, agonist treatment induced a strong decrease in the abundance of all peptides, independently of their phosphorylation status (Table 1). One hypothesis is that additional modifications occur in this region upon agonist treatment, leading to peptides no longer detectable using our technique. New database searches considering variable ubiquitinated lysine modification did not reveal the presence of this

FIGURE 2. **MS/MS analysis of human NPFF$_2$ receptor phosphorylation.** *A*, isolation of NPFF$_2$ receptors. On the *left* is shown a representative GFP Western blot after hNPFF$_2$-YFP receptor immunoprecipitation. On the *right* is shown a representative Coomassie-stained gel obtained from the immunoprecipitated sample. The *dotted line* delimits the gel piece that was cut and trypsin-digested for nanoLC-MS/MS analysis. *B*, representative Coomassie-stained gel showing the 36-kDa band corresponding to the GST-thrombin-hNPFF$_2$ C terminus fusion protein. *C*, the CID MS/MS spectrum of the diphosphorylated peptide, ^{369}SHVLINpTpSNQLVQESTFQNPHGETLLYR^{396} (triply charged precursor ion, MH^{3+}, at *m/z* 1129.1885) displays series of b- and y-ions, indicating that Thr^{375} and Ser^{376} are phosphorylated. Sequence and phosphorylated position are indicated. *D*, the ETD MS/MS spectrum of the monophosphorylated peptide, ^{397}pSAEKPQQELVMEELK^{412} (triply charged precursor ion, MH3+, at *m/z* 613.6251) displays series of c- and z-ions, indicating that Ser^{398} is phosphorylated. Sequence and phosphorylated position are indicated.

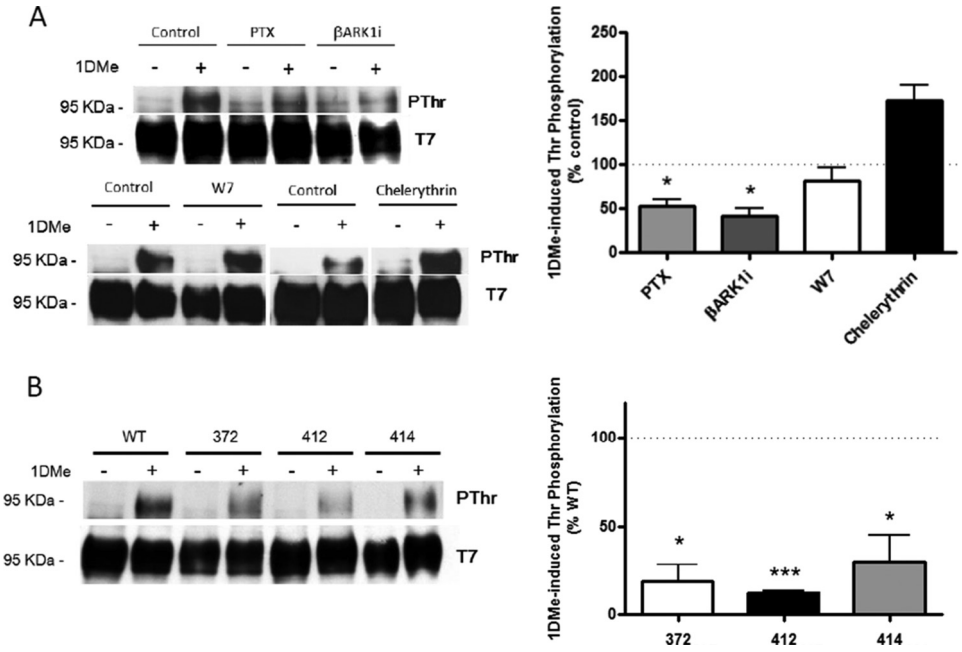

FIGURE 3. **Western blot analysis of NPFF$_2$ receptor phosphorylation on threonines.** *A*, *left panel*, representative Western blots showing 1DMe-induced WT NPFF$_2$ receptor phosphorylation on threonines in the absence or presence of G protein or kinase inhibitors. Cells were treated with 1 μM 1DMe for 30 min, receptors were immunoprecipitated using anti-T7 tag antibodies and phosphorylation detected using anti-phosphothreonine antibodies as described under "Experimental Procedures." *PThr*, anti-PThr antibody; *T7*, anti-T7 tag antibody; *βARK1i*, GRK2 inhibitor. *Right panel*, quantification of 1DMe-induced phosphorylation. The results were normalized to the total amount of immunoprecipitated receptors (anti-T7 WB) and are expressed as a percentage of the phosphorylation induced in the absence of inhibitors. The values are means ± S.E. of three or four independent experiments. *, $p < 0.05$, one sample *t* test compared with 100. *B*, *left panel*, representative Western blot showing 1DMe-induced receptor phosphorylation on threonines on WT and mutant NPFF$_2$ receptors. *Right panel*, quantification of three independent experiments. Experiment, quantification, and statistics were performed as in *A* except that the results are expressed as percentages of the 1DMe-induced phosphorylation of WT receptors. ***, $p < 0.001$.

kind of post-translational modification in the hNPFF$_2$ receptor C terminus. Alternatively, a strong heterogeneous polyphosphorylation could produce a large number of differentially phosphorylated peptides, each of them falling below the detection limit of our analysis.

By using the GPS software (34) to predict putative kinase consensus sites on the hNPFF$_2$ receptor, we found a high score for GRK2 at the TTNSS cluster. This was further confirmed by *in vitro* phosphorylation experiments with the purified kinase. GRK2 and the receptor C terminus (last 85 amino acids) fused to GST were mixed for 2 h in the presence of ATP, and the receptor fragment was then isolated by SDS-PAGE (Fig. 2*B*). The trypsin digest was analyzed by nanoLC-MS/MS similarly to the full size receptor. The list of the identified phosphorylated peptides is given in Table 1. As predicted by the consensus sequence search, GRK2 phosphorylation was restricted to the TTNSS cluster. Peptides bearing a single phosphorylation on Thr^{414}, Thr^{415}, Ser^{417}, or Ser^{418} and a dual phosphorylation on Thr^{415} and Ser^{417} or Ser^{418} were identified, confirming our suspicion of a possible heterogeneous polyphosphorylation in this cluster.

Taken together, these MS/MS analyses identified phosphorylation sites only in the C-terminal tail of the hNPFF$_2$ receptor. Except for Ser^{369}, all of these residues are conserved between human and rat (Fig. 1*B*). Therefore, in the second part of the study, these amino acids were mutated to alanine in the rat NPFF$_2$ receptor to evaluate their function in the regulation of receptor signaling and trafficking (Fig. 1*B*). Thr^{372} and Ser^{373} (corresponding to Thr^{375} and Ser^{376} in human) were mutated in the TS372AA construct (called 372 in the simplified nomenclature). Ser^{395} (Ser^{398} in human) was substituted in the S395A mutant (395). Ser^{414} and Thr^{415} (Ser^{417} and Thr^{418} in human) were replaced by alanine in the ST414AA construct (414), whereas the whole TNST cluster was replaced in the TNST412ANAA mutant (412). Finally, two residues, Ser^{382} and Ser^{386}, absent from the human sequence but suspected to be phosphorylated in preliminary MS experiments on the rat receptor, were also substituted by alanine in the S382A/S386A double mutant (382).

Western Blot Analysis of the Rat NPFF$_2$ Receptor Phosphorylation on Threonines—Before studying the role of each set of phosphorylated residues, we used a second approach to monitor the rat receptor phosphorylation. Cells were treated with or without 1 μM 1DMe, and receptors were immunoprecipitated using anti-T7 tag antibodies. Serine residue phosphorylation could not be studied because of the lack of efficient antibodies. In contrast, we identified an anti-phosphothreonine antibody (Invitrogen), which detected a strong increase in receptor phosphorylation after 1DMe treatment (Fig. 3*A*). Phosphorylation was maximal after 20 min of treatment and was then stable for at least 1 h (data not shown). It was partly inhibited in cells that had been treated overnight with PTX, indicating that the activation of heterotrimeric $G_{i/o}$ proteins by the receptor was necessary for its optimal phosphorylation. Receptor phosphorylation was also strongly reduced by a GRK2 inhibitor (*β*ARK1i), confirming our *in vitro* MS data, which suggested that the receptor could be a GRK2 substrate. On the contrary, 1DMe-induced phosphorylation was unaffected or tended to increase

TABLE 2

Binding properties of 1DMe in cells expressing WT and mutant rNPFF$_2$ receptors

The results are expressed as means ± S.E. of at least three independent experiments performed in duplicate.

	[^{3}H]EYF binding	
	K_D	B_{max}
	nM	*pmol/mg*
WT	4.1 ± 0.4	7.4 ± 0.4
372	2.0 ± 0.2[a]	4.1 ± 0.3
382	1.9 ± 0.4	1.5 ± 0.7
395	5.5 ± 2	9.7 ± 3
414	5.2 ± 1	13.2 ± 3
412	4.0 ± 0.8	3.3 ± 0.7

[a] $p < 0.05$ compared to WT, unpaired Student's *t* test.

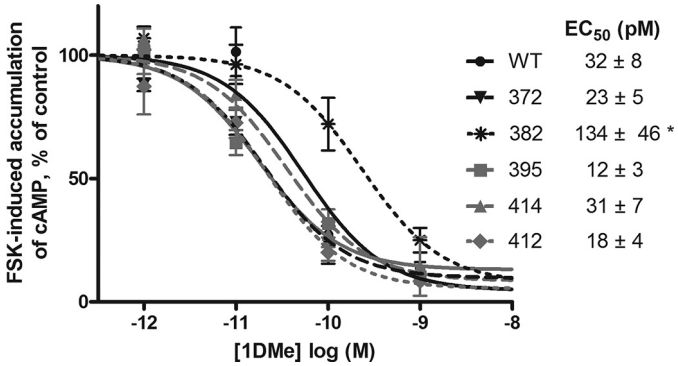

FIGURE 4. **Adenylyl cyclase inhibition following NPFF$_2$ receptor activation.** Inhibition by 1DMe of forskolin (*FSK*)-induced cAMP accumulation in recombinant SH-SY5Y cells expressing the WT and the different mutant rat NPFF$_2$ receptors. Cells were treated with FSK ± 1DMe for 10 min, and cAMP contents were evaluated as described under "Experimental Procedures." Control refers to accumulated cAMP in the absence of agonist. Each point represents the mean ± S.E. of at least three independent experiments performed in duplicate. *, $p < 0.05$ compared with WT, unpaired Student's *t* test.

in the presence of W7 or chelerythrin, respectively, ruling out the involvement of calmodulin kinase or PKC isoforms in this process. Finally, after normalization to the total amount of immunoprecipitated receptors, threonine phosphorylation following activation appeared to be strongly reduced in all threonine mutants, namely 372, 414, and 412 mutant receptors (Fig. 3*B*). This confirms that, as suggested by MS analysis of the human receptor, agonist treatment induces the phosphorylation of three conserved threonines in the rat NPFF$_2$ receptor: Thr^{372} in the ^{372}TS^{373} doublet and Thr^{412} and Thr^{415} in the ^{412}TNST^{415} cluster.

The Loss of Phosphorylation Sites Has a Minor Impact on NPFF$_2$ Receptor Acute Signaling—Saturation binding experiments using [^{3}H]EYF on membrane preparations from stable SH-SY5Y cell lines expressing WT or mutant rNPFF$_2$ receptors revealed that removal of phosphorylation sites does not affect receptor affinity for the agonist except for mutant 372, which showed a small but significant 2-fold decrease in K_d (Table 2). Expression levels of the various constructs were in the picomolar range (from 1.5 to 13.2 pmol/mg of membrane proteins). cAMP assays were then performed as a first test of the signaling properties of mutant receptors (Fig. 4). All receptors were able to fully inhibit forskolin-induced cAMP accumulation. 1DMe inhibited cAMP production with a similar high potency in cells expressing mutant receptors except for the 382 mutant, which showed a small but significant 4-fold reduction in agonist potency. We then studied ERK activation to investigate another pathway located more downstream of NPFF$_2$ receptor signaling. As shown in Fig. 5, treatment of SH-SY5Y cells expressing WT receptors with 1 μM 1DMe for up to 30 min induced a sustained increase in ERK1 and ERK2 phosphorylation. Pretreating the cells with PTX (100 ng/ml) for 18 h fully inhibited the effect of 1DMe, indicating that $G_{i/o}$ protein activity is required to promote ERK phosphorylation, even at late time points (Fig. 5*B*). Compared with the WT receptor, mutants did not show any significant difference in their ability to induce ERK phosphorylation at any time point (two-way analysis of variance followed by Bonferroni post hoc tests). Although experimental variability might have prevented us from detecting subtle changes, this result suggests that phosphorylation of the mutated residues is not involved in the regulation of NPFF$_2$-dependent ERK signaling. Overall these results show that no individual phosphorylation site/cluster is mandatory for $G_{i/o}$-dependent NPFF$_2$ receptor signaling.

Role of Phosphorylation Sites in NPFF$_2$ Receptor Desensitization—The ability of NPFF$_2$ receptor activation to induce intracellular calcium release was used to study acute receptor desensitization. Treatment of cells expressing the WT rat NPFF$_2$ receptor with 1 μM 1DMe induced a strong increase in intracytoplasmic calcium ($[Ca^{2+}]_i$), as measured using the Fluo4-AM fluorescent probe. This effect was sensitive to PTX pretreatment (data not shown). Calcium levels progressively decreased over the course of 1DMe perfusion, going back to baseline levels after 5 min (Fig. 6*A*). This decrease was for most part due to homologous desensitization because cells were still responsive to the muscarinic agonist carbachol after 3 and 5 min of 1DMe perfusion (data not shown). The desensitization profile was different between WT and several mutant receptors (Fig. 6*A*). To quantify the desensitization properties of the WT and mutant receptors, we determined the amount of $[Ca^{2+}]_i$ signal remaining after 2.5 and 5 min of 1DMe perfusion (Fig. 6, *B* and *C*, respectively). The 372 mutant showed a slower desensitization, with a decrease in response that was significantly different from WT after 2.5 but not 5 min of treatment. The desensitization of the 414 and 412 mutants was also impaired, with a $[Ca^{2+}]_i$ signal remaining ~50% above basal values after 5 min of 1DMe perfusion. To confirm these results, we used a different desensitization paradigm based on two stimulations with 1DMe for 1 min, separated by 10 min of washing. In cells expressing WT receptors, 1DMe lost ~85% of its maximal effect between the two stimulations (Fig. 6*D*). In contrast, carbachol was still active (data not shown), indicating again that we were monitoring homologous desensitization. Among all modified receptors, only the 414 and 412 mutants conserved an activity significantly higher than that of the WT in response to the second 1DMe treatment. Overall these data identified the ^{372}TS^{373} and ^{412}TNST^{415} phosphorylation clusters as being involved in acute NPFF$_2$ receptor desensitization, with Ser^{414} and Thr^{415} playing the major role.

Role of Phosphorylation Sites in NPFF$_2$ Receptor Internalization—We next studied WT and mutant NPFF$_2$ receptor internalization following exposure to 1 μM 1DMe for 30 min. As shown in Fig. 7, 1DMe treatment induced a strong internaliza-

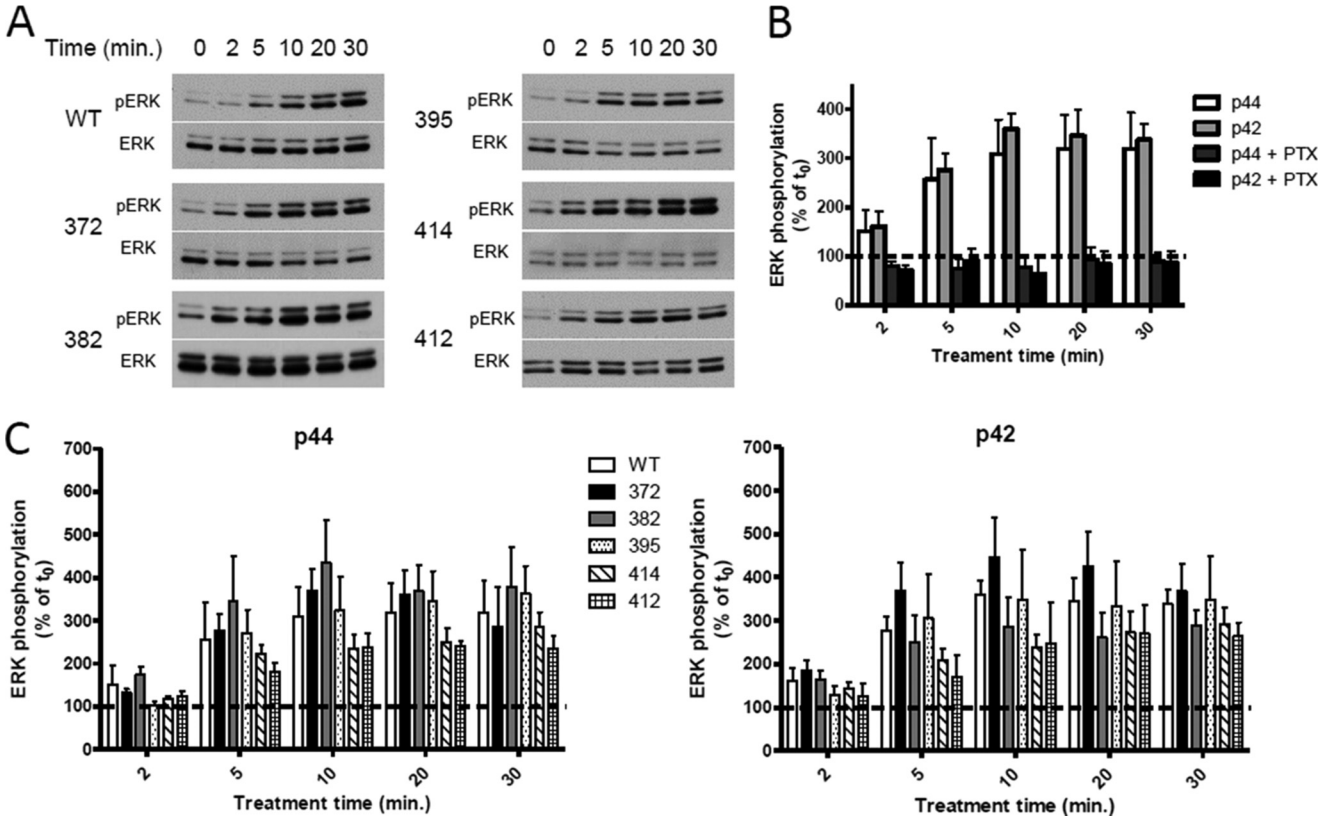

FIGURE 5. **ERK1/2 activation induced by NPFF$_2$ receptor activation.** *A*, representative Western blots showing 1DMe-induced ERK activation in SH-SY5Y cells expressing WT and mutant NPFF$_2$ receptors. Cells were treated with 1 μM 1DMe for the indicated time and phosphorylated (pERK), and total ERK 1 and 2 were detected as described under "Experimental Procedures." *B*, quantification of 1DMe-induced ERK phosphorylation in cells expressing WT receptors pretreated or not with PTX (100 ng/ml, 18 h). The results were normalized to the total amount of ERK and are expressed as percentages of the basal phosphorylation at time 0. *C*, quantification 1DMe-induced ERK phosphorylation in cells expressing WT or mutant NPFF$_2$ receptors. The results are expressed as in *B*. The values are means ± S.E. of three or four independent experiments. *p44*, ERK1; *p42*, ERK2.

tion of the WT receptor, which tended to disappear from the plasma membrane and was found in intracellular vesicles after 30 min (46% decrease in normalized membrane level). This effect was significantly inhibited by PTX pretreatment (63% inhibition), indicating that $G_{i/o}$ protein activation also contributed to receptor trafficking, in addition to receptor phosphorylation. All mutant receptors showed a trend for a lower level of internalization after 30 min of 1DMe. However, the impairment was only significant for mutant receptors 395 (74% inhibition), 414 (72%) and 412 (78%) (Fig. 7). The ^{412}TNST^{415} cluster thus appears to be important for both desensitization and internalization. In contrast, the ^{372}TS^{373} doublet contributes to desensitization without playing a major role in internalization, whereas Ser^{395} phosphorylation is only necessary for efficient internalization.

The phosphorylation of GPCR C terminus contributes to internalization through the recruitment of β-arrestins. We thus monitored this recruitment by transiently transfecting β-arrestin2-GFP in our cells. GFP fluorescence was homogeneously distributed in the cytoplasm in control cells (Fig. 8). Activation of WT receptors induced a strong clustering of β-arrestin2-GFP, resulting in the detection of numerous intracellular fluorescent punctae after 30 min of 1DMe treatment. β-Arrestin2 recruitment was also evident in mutant receptors. However, in cells expressing the internalization-deficient mutant receptors 395 and 414, β-arrestin2 fluorescence was present at the plasma membrane in addition to intracellular vesicles (Fig. 8), indicating that although it is recruited, the protein is less efficient in promoting internalization.

DISCUSSION

In this study, we combined mass spectrometric analysis and site-directed mutagenesis to analyze for the first time the phosphorylation pattern of the human and rat NPFF$_2$ receptors and the role of the various phosphorylation sites in rat receptor signaling, desensitization, and trafficking in a SH-SY5Y model cell line. More precisely, we identified the major, likely GRK-dependent, phosphorylation cluster responsible for acute desensitization: ^{412}TNST^{415} at the end of the C terminus of the receptor. In addition, our study is the first to fully characterize rat receptor signaling.

In our cell model, NPFF$_2$ receptors appear to couple to PTX-sensitive $G_{i/o}$ proteins to inhibit adenylyl cyclase, induce intracellular calcium release, and activate ERK1/2. Negative coupling to adenylyl cyclase is consistent with what has been described for human and mouse receptors (35, 36). However, the potency of 1DMe is increased by more than 1 order of magnitude in the rat species. ERK activation by NPFF$_2$ receptors has been demonstrated previously in rat and human cell lines that were shown to endogenously express the receptor (14, 37, 38). Here we confirm the specificity of this effect by using recombinant cells. We also show that ERK activation by 1DMe lasts for

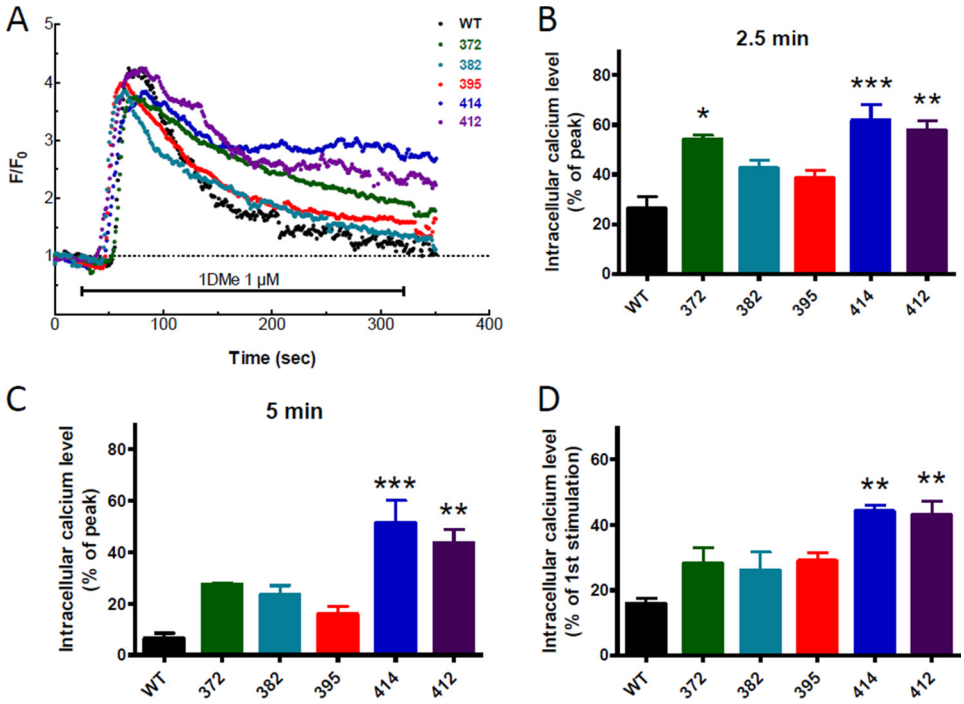

FIGURE 6. **Desensitization of 1DMe-induced intracellular calcium release.** *A*, representative traces showing intracellular calcium release during 5 min of treatment with 1 μM 1DMe in cells expressing WT or mutant NPFF$_2$ receptors. Calcium levels were monitored using the fluorescent Ca^{2+} indicator Fluo-4-AM, and fluorescence intensity was normalized using the average intensity measured during 20 s before addition of the agonist (F/F_0). *B* and *C*, intracellular calcium level after 2.5 and 5 min of 1DMe treatment, respectively, compared with the peak of release. *D*, response to 1 min treatment with 1 μM 1DMe compared with the response to a first stimulation performed 10 min before. The values are means ± S.E. of three or four independent experiments. *, $p < 0.05$; **, $p < 0.01$; ***, $p < 0.001$ compared with WT; one-way analysis of variance followed by Bonferroni post hoc tests.

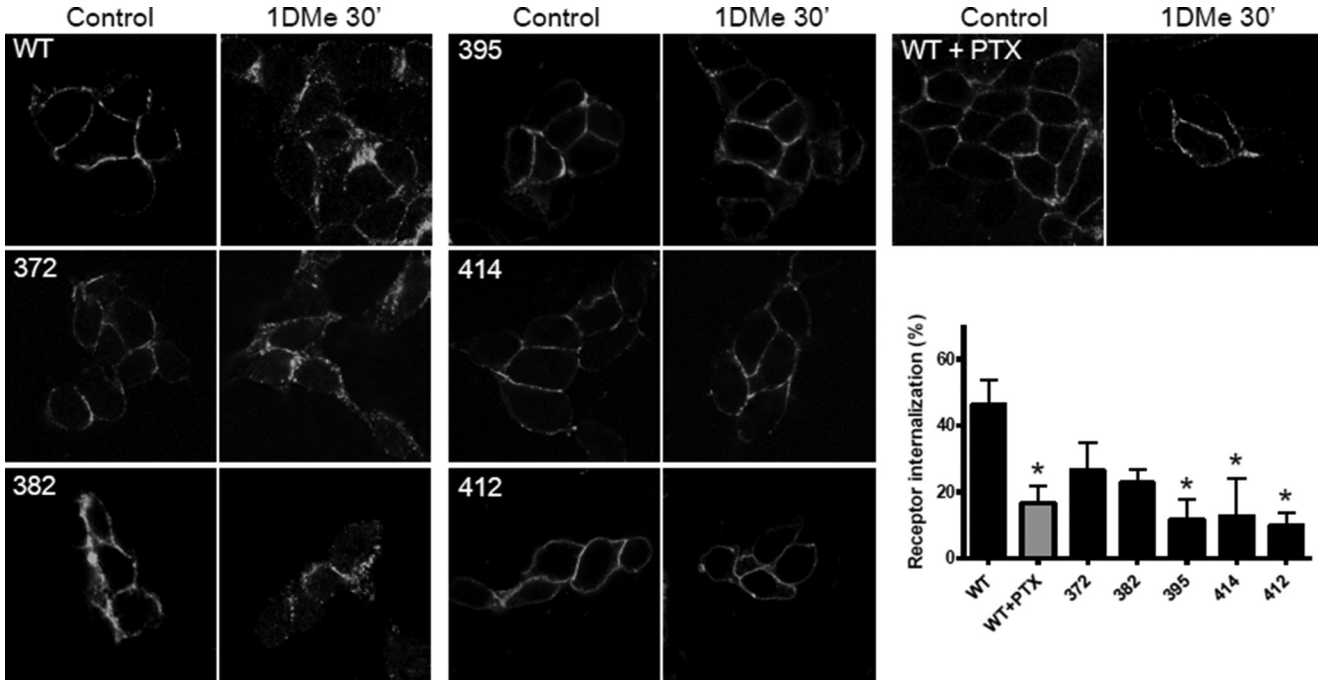

FIGURE 7. **1DMe-induced receptor internalization.** Representative confocal images of receptor internalization. Cells expressing WT or mutant NPFF$_2$ receptors were treated with 1 μM 1DMe for 30 min at room temperature before formaldehyde fixation and anti-T7 immunofluorescence. Confocal images were taken with a laser scanner confocal microscope and quantified as described under "Experimental Procedures." The results in the histogram are expressed as means ± S.E. of at least three independent experiments. *, $p < 0.05$ compared with WT; one-way analysis of variance followed by Bonferroni post hoc tests.

at least 30 min. Similarly to several other $G_{i/o}$-coupled receptors (39), ERK activation appears to be PTX-sensitive and thus fully dependent on G protein activation. The involvement of β-arrestins in the late phase of ERK phosphorylation remains to be tested. Finally, to the best of our knowledge, our study is the first one to demonstrate a direct effect of NPFF$_2$ receptor activation on intracellular calcium release without the need for concomitant activation of a G_q-coupled receptor (31).

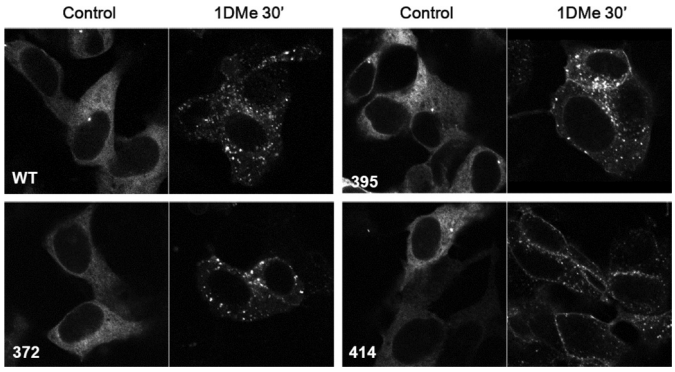

FIGURE 8. **1DMe-induced β-arrestin2 recruitment.** Representative confocal images of β-arrestin2-GFP distribution. Cells expressing WT or mutant NPFF$_2$ receptors were transiently transfected with β-arrestin2-GFP and treated 48 h post-transfection with 1 μM 1DMe for 30 min at room temperature before formaldehyde fixation and imaging of the GFP fluorescence. Confocal images were taken with a laser scanner confocal microscope as described under "Experimental Procedures."

A mass spectrometry strategy was used to map the phosphorylated residues in the human and rat NPFF$_2$ receptors. The high sequence coverage obtained with the human receptor enabled us to study all the putative phosphorylation sites, except Thr^{157} in the second intracellular loop. Because Western blot data showed that threonine phosphorylation is strongly reduced by mutation of Thr^{372}, Thr^{412}, and Thr^{415} to alanine, we can assume that Thr^{157} is not phosphorylated. We can thus conclude that among 19 putative phosphorylation sites in the human receptor intracellular domain, only eight residues, located in the C-terminal part, can be phosphorylated either in the basal state or after agonist treatment. Six residues are conserved in the rat (and also the mouse) sequence (Fig. 2): Thr^{372} (375 in human), Ser^{373} (376), Ser^{395} (398), Thr^{412} (415), Ser^{414} (417), and Thr^{415} (Ser^{418}). Intriguingly, although these conserved phosphorylation sites represent the best candidates for mediating NPFF$_2$ receptor regulation, species specific sites were also identified in human (Ser^{369}) and rat (Ser^{382} and Ser^{386}). The rat-specific residues did not play a significant role in receptor desensitization and internalization, but as discussed above, they might contribute to subtle species differences in G protein coupling. Once phosphorylation sites are identified, an important question is whether these modifications are present in the basal state or result from receptor activation. Label-free relative quantification of the MS data clearly indicated that the phosphorylation of Thr^{375} and Ser^{376} is increased in the human receptor after 1DMe treatment. Unfortunately, technical limitations did not allow us to confidently quantify the effect of agonist treatment on the remaining four conserved residues. However, *in vitro* experiments using purified GRK2 and the human NPFF$_2$ receptor C terminus fused to GST suggested that the 414–418 cluster is a GRK substrate, in agreement with the presence of acidic amino acid in both the N and C termini of this region (40). Taken together our MS data support the agonist-induced phosphorylation of the ^{414}TTNSS^{418} by GRK2 and of the ^{375}TS^{376} doublet by an unknown kinase in the human NPFF$_2$ receptor.

Agonist-induced phosphorylation of these two loci was confirmed in the rat sequence using anti-phosphothreonine antibodies. Mutating Thr^{372}, Thr^{412}, and/or Thr^{415} to alanine strongly reduced the amount of phosphothreonine after 1DMe treatment. In agreement with the *in vitro* data, part of this phosphorylation was prevented in the presence of a GRK2 inhibitor. We also showed by using PTX that G protein activation contributed to agonist induced phosphorylation. GPS analysis (34) of the sequence surrounding Thr^{372} revealed that the best candidates to phosphorylate this residue were PKC and calmodulin kinase. However, the calmodulin inhibitor W7 and the PKC inhibitor chelerythrin did not reduce phosphorylation of receptor threonines. On the contrary, chelerythrin tended to increase it, maybe by counteracting the inhibitory effect of PKC on a kinase responsible for receptor phosphorylation. Because PKC is known to inhibit GRK5 activity (41), the latter could thus be suspected to phosphorylate the ^{372}TS^{373} doublet. Therefore, GRKs could mediate agonist-induced phosphorylation of both the ^{372}TS^{373} doublet and the ^{412}TNST^{415} cluster. G protein activation could contribute to this effect via the Gα subunit for GRK5/6 (42) and the Gβγ subunits in the case of GRK2/3 (43). siRNA knockdown of each GRK subtype should be combined with the analysis of the phosphorylation of individual threonine mutants to confirm these hypothesis.

The removal of individual conserved phosphorylation sites did not strongly affect NPFF$_2$ receptor signaling. Most mutant receptors remained able to activate $G_{i/o}$-dependent signaling pathways with equivalent potency, indicating that NPFF$_2$ receptor phosphorylation is mainly involved in receptor regulation following G protein activation. However, the 382 mutant showed a 4-fold decrease in potency in the cAMP assay. This suggests that the phosphorylation of Ser^{386}, present only in the rat sequence, could be in part responsible for the increase in potency observed for the rat receptor compared with its human and mouse counterparts, as mentioned above. One might also suggest that the lower potency of the 382 mutant is due to its lower expression level. However, this explanation appears unlikely because the B_{max} of the 412 mutant is also more than 2-fold lower than that of the WT, whereas its potency is not lower, demonstrating that there is no correlation between EC_{50} and B_{max} in the cAMP assay under our experimental conditions.

Two agonist-regulated phosphorylation loci were found implicated in acute receptor desensitization. Mutation of the ^{372}TS^{373} doublet significantly slowed down desensitization. However, the main phosphorylation site responsible for receptor desensitization appears to be the ^{412}TNST^{415} cluster at the extreme C terminus that we identified as a GRK2 phosphorylation site *in vitro*. Alanine mutation within this cluster had a strong impact on desensitization, similar for the 412 and 414 mutants, suggesting that the principal residues responsible for homologous desensitization of the NPFF$_2$ receptor are Ser^{414} and Thr^{415}. Again, the observed changes cannot be attributed to changes in expression level because they are similar for the two mutants, whereas their B_{max} are twice lower (412) and twice higher (414) than that of the WT receptor.

Agonist-induced receptor internalization was affected by alanine mutation of some sites or clusters, but there was no direct correlation between the behavior of a given mutant in terms of desensitization and of internalization. The ^{412}TNST^{415} cluster played a major role in both events, whereas

preventing phosphorylation of the ^{372}TS^{373} doublet had a significant effect on desensitization but did not significantly affect internalization. On the contrary, the S395A mutant desensitized normally but showed impaired internalization. This is in agreement with previous data showing that residues involved in GPCR desensitization and internalization do not strictly overlap (44–47). Thus in contrast with desensitization, which depends on the phosphorylation of a particular cluster, our data confirm the lack of a "master" phosphorylation event (48) sufficient to trigger GPCR internalization. The case of the mu opioid receptor offers a good illustration of this concept. The main desensitizing event is the phosphorylation of a single residue, Ser^{375} located in a STANT phosphorylation cluster near the end of the receptor C terminus. However, this modification is necessary but not sufficient to induce internalization. Agonists such as morphine, which induce Ser^{375} phosphorylation but do not efficiently trigger the phosphorylation of additional residues in the C terminus, produce desensitization without significant internalization (49). As previously shown for the human receptor (2, 18), we show here that the rat NPFF$_2$ receptor activation induces the recruitment of β-arrestin2. The interaction of arrestin with GPCR depends in part on phosphorylated residues in the C terminus making individual contacts with the scaffolding protein, each contributing to the stability and the conformation of the complex (24, 50). It is thus probable that each of our mutants, despite having retained the ability to recruit β-arrestin2, interacts with the scaffolding protein with lower affinity, thus reducing the efficiency of the internalization process.

In conclusion, the present work identified the phosphorylation pattern of NPFF$_2$ receptors. Further characterization of the residues involved in desensitization (^{412}TNST^{415} cluster and ^{372}TS^{373} doublet) and internalization (^{412}TNST^{415} cluster and Ser^{395}) of the receptor indicated that these two regulatory processes do not rely on strictly overlapping post-translational modifications. Finally, Ser^{414} and Thr^{415} appear to be the best candidates to develop phospho-specific antibodies to detect activated NPFF$_2$ receptors.

Acknowledgments—We thank Dr. S. Krief for providing the rat NPFF$_2$ receptor, Prof. J. Benovic (Thomas Jefferson University, Philadelphia, PA) for providing purified GRK2 protein, and Dr. S. Allouche (Université de Caen, Caen, France) for providing β-arrestin2-GFP.

REFERENCES

1. Bonini, J. A., Jones, K. A., Adham, N., Forray, C., Artymyshyn, R., Durkin, M. M., Smith, K. E., Tamm, J. A., Boteju, L. W., Lakhlani, P. P., Raddatz, R., Yao, W. J., Ogozalek, K. L., Boyle, N., Kouranova, E. V., Quan, Y., Vaysse, P. J., Wetzel, J. M., Branchek, T. A., Gerald, C., and Borowsky, B. (2000) Identification and characterization of two G protein-coupled receptors for neuropeptide FF. *J. Biol. Chem.* **275,** 39324–39331
2. Elshourbagy, N. A., Ames, R. S., Fitzgerald, L. R., Foley, J. J., Chambers, J. K., Szekeres, P. G., Evans, N. A., Schmidt, D. B., Buckley, P. T., Dytko, G. M., Murdock, P. R., Milligan, G., Groarke, D. A., Tan, K. B., Shabon, U., Nuthulaganti, P., Wang, D. Y., Wilson, S., Bergsma, D. J., and Sarau, H. M. (2000) Receptor for the pain modulatory neuropeptides FF and AF is an orphan G protein-coupled receptor. *J. Biol. Chem.* **275,** 25965–25971
3. Zajac, J. M. (2001) Neuropeptide FF: new molecular insights. *Trends Pharmacol. Sci.* **22,** 63
4. Panula, P., Aarnisalo, A. A., and Wasowicz, K. (1996) Neuropeptide FF, a mammalian neuropeptide with multiple functions. *Prog. Neurobiol.* **48,** 461–487
5. Mollereau, C., Roumy, M., and Zajac, J. M. (2005) Opioid-modulating peptides: mechanisms of action. *Curr. Top. Med. Chem.* **5,** 341–355
6. Moulédous, L., Mollereau, C., and Zajac, J. M. (2010) Opioid-modulating properties of the neuropeptide FF system. *Biofactors* **36,** 423–429
7. Yang, H. Y., Tao, T., and Iadarola, M. J. (2008) Modulatory role of neuropeptide FF system in nociception and opiate analgesia. *Neuropeptides* **42,** 1–18
8. Simonin, F., Schmitt, M., Laulin, J. P., Laboureyras, E., Jhamandas, J. H., MacTavish, D., Matifas, A., Mollereau, C., Laurent, P., Parmentier, M., Kieffer, B. L., Bourguignon, J. J., and Simonnet, G. (2006) RF9, a potent and selective neuropeptide FF receptor antagonist, prevents opioid-induced tolerance associated with hyperalgesia. *Proc. Natl. Acad. Sci. U.S.A.* **103,** 466–471
9. Elhabazi, K., Trigo, J. M., Mollereau, C., Moulédous, L., Zajac, J. M., Bihel, F., Schmitt, M., Bourguignon, J. J., Meziane, H., Petit-Demoulière, B., Bockel, F., Maldonado, R., and Simonin, F. (2012) Involvement of neuropeptide FF receptors in neuroadaptative responses to acute and chronic opiate treatments. *Br. J. Pharmacol.* **165,** 424–435
10. Kotani, M., Mollereau, C., Detheux, M., Le Poul, E., Brézillon, S., Vakili, J., Mazarguil, H., Vassart, G., Zajac, J. M., and Parmentier, M. (2001) Functional characterization of a human receptor for neuropeptide FF and related peptides. *Br. J. Pharmacol.* **133,** 138–144
11. Mollereau, C., Zajac, J. M., and Roumy, M. (2007) Staurosporine differentiation of NPFF(2) receptor-transfected SH-SY5Y neuroblastoma cells induces selectivity of NPFF activity towards opioid receptors. *Peptides* **28,** 1125–1128
12. Pertovaara, A., Ostergård, M., Ankö, M. L., Lehti-Koivunen, S., Brandt, A., Hong, W., Korpi, E. R., and Panula, P. (2005) RFamide-related peptides signal through the neuropeptide FF receptor and regulate pain-related responses in the rat. *Neuroscience* **134,** 1023–1032
13. Mollereau, C., Roumy, M., and Zajac, J. M. (2011) Neuropeptide FF receptor modulates potassium currents in a dorsal root ganglion cell line. *Pharmacol. Rep.* **63,** 1061–1065
14. Ankö, M. L., and Panula, P. (2006) Regulation of endogenous human NPFF2 receptor by neuropeptide FF in SK-N-MC neuroblastoma cell line. *J. Neurochem.* **96,** 573–584
15. Chuang, T. T., Iacovelli, L., Sallese, M., and De Blasi, A. (1996) G protein-coupled receptors: heterologous regulation of homologous desensitization and its implications. *Trends Pharmacol. Sci.* **17,** 416–421
16. Lohse, M. J. (1993) Molecular mechanisms of membrane receptor desensitization. *Biochim. Biophys. Acta* **1179,** 171–188
17. Hüttenrauch, F., Pollok-Kopp, B., and Oppermann, M. (2005) G protein-coupled receptor kinases promote phosphorylation and β-arrestin-mediated internalization of CCR5 homo- and hetero-oligomers. *J. Biol. Chem.* **280,** 37503–37515
18. Moulédous, L., Froment, C., Dauvillier, S., Burlet-Schiltz, O., Zajac, J. M., and Mollereau, C. (2012) GRK2-mediated trans-phosphorylation contributes to the loss of function of mu opioid receptors induced by neuropeptide FF (NPFF2) receptors. *J. Biol. Chem.* **287,** 12736–12749
19. Gainetdinov, R. R., Premont, R. T., Bohn, L. M., Lefkowitz, R. J., and Caron, M. G. (2004) Desensitization of G protein-coupled receptors and neuronal functions. *Annu. Rev. Neurosci.* **27,** 107–144
20. Shenoy, S. K., and Lefkowitz, R. J. (2011) β-Arrestin-mediated receptor trafficking and signal transduction. *Trends Pharmacol. Sci.* **32,** 521–533
21. Busillo, J. M., Armando, S., Sengupta, R., Meucci, O., Bouvier, M., and Benovic, J. L. (2010) Site-specific phosphorylation of CXCR4 is dynamically regulated by multiple kinases and results in differential modulation of CXCR4 signaling. *J. Biol. Chem.* **285,** 7805–7817
22. Butcher, A. J., Prihandoko, R., Kong, K. C., McWilliams, P., Edwards, J. M., Bottrill, A., Mistry, S., and Tobin, A. B. (2011) Differential G-protein-coupled receptor phosphorylation provides evidence for a signaling bar code. *J. Biol. Chem.* **286,** 11506–11518
23. Lau, E. K., Trester-Zedlitz, M., Trinidad, J. C., Kotowski, S. J., Krutchinsky, A. N., Burlingame, A. L., and von Zastrow, M. (2011) Quantitative encoding of the effect of a partial agonist on individual opioid receptors by

multisite phosphorylation and threshold detection. *Sci. Signal* **4,** ra52
24. Nobles, K. N., Xiao, K., Ahn, S., Shukla, A. K., Lam, C. M., Rajagopal, S., Strachan, R. T., Huang, T. Y., Bressler, E. A., Hara, M. R., Shenoy, S. K., Gygi, S. P., and Lefkowitz, R. J. (2011) Distinct phosphorylation sites on the β2-adrenergic receptor establish a barcode that encodes differential functions of β-arrestin. *Sci. Signal.* **4,** ra51
25. Liggett, S. B. (2011) Phosphorylation barcoding as a mechanism of directing GPCR signaling. *Sci. Signal.* **4,** pe36
26. Tobin, A. B., Butcher, A. J., and Kong, K. C. (2008) Location, location, location: site-specific GPCR phosphorylation offers a mechanism for cell-type-specific signalling. *Trends Pharmacol. Sci.* **29,** 413–420
27. Gluck, L., Loktev, A., Mouledous, L., Mollereau, C., Law, P. Y., and Schulz, S. (2014) Loss of morphine reward and dependence in mice lacking G protein-coupled receptor kinase 5. *Biol. Psychiatry* **2014,** pii
28. Gicquel, S., Mazarguil, H., Allard, M., Simonnet, G., and Zajac, J. M. (1992) Analogues of F8Famide resistant to degradation, with high affinity and in vivo effects. *Eur. J. Pharmacol.* **222,** 61–67
29. Talmont, F., Garcia, L. P., Mazarguil, H., Zajac, J. M., and Mollereau, C. (2009) Characterization of two novel tritiated radioligands for labelling Neuropeptide FF (NPFF$_1$ and NPFF$_2$) receptors. *Neurochem. Int.* **55,** 815–819
30. Moulédous, L., Merker, S., Neasta, J., Roux, B., Zajac, J. M., and Mollereau, C. (2008) Neuropeptide FF-sensitive confinement of mu opioid receptor does not involve lipid rafts in SH-SY5Y cells. *Biochem. Biophys. Res. Commun.* **373,** 80–84
31. Mollereau, C., Mazarguil, H., Zajac, J. M., and Roumy, M. (2005) Neuropeptide FF (NPFF) analogs functionally antagonize opioid activities in NPFF2 receptor-transfected SH-SY5Y neuroblastoma cells. *Mol. Pharmacol.* **67,** 965–975
32. Taus, T., Köcher, T., Pichler, P., Paschke, C., Schmidt, A., Henrich, C., and Mechtler, K. (2011) Universal and confident phosphorylation site localization using phosphoRS. *J. Proteome Res.* **10,** 5354–5362
33. Gautier, V., Mouton-Barbosa, E., Bouyssié, D., Delcourt, N., Beau, M., Girard, J. P., Cayrol, C., Burlet-Schiltz, O., Monsarrat, B., and Gonzalez de Peredo, A. (2012) Label-free quantification and shotgun analysis of complex proteomes by one-dimensional SDS-PAGE/NanoLC-MS: evaluation for the large scale analysis of inflammatory human endothelial cells. *Mol. Cell. Proteomics* **11,** 527–539
34. Xue, Y., Ren, J., Gao, X., Jin, C., Wen, L., and Yao, X. (2008) GPS 2.0, a tool to predict kinase-specific phosphorylation sites in hierarchy. *Mol. Cell. Proteomics* **7,** 1598–1608
35. Mollereau, C., Mazarguil, H., Marcus, D., Quelven, I., Kotani, M., Lannoy, V., Dumont, Y., Quirion, R., Detheux, M., Parmentier, M., and Zajac, J. M. (2002) Pharmacological characterization of human NPFF$_1$ and NPFF$_2$ receptors expressed in CHO cells by using NPY Y$_1$ receptor antagonists. *Eur. J. Pharmacol.* **451,** 245–256
36. Talmont, F., Moulédous, L., Piedra-Garcia, L., Schmitt, M., Bihel, F., Bourguignon, J. J., Zajac, J. M., and Mollereau, C. (2010) Pharmacological characterization of the mouse NPFF2 receptor. *Peptides* **31,** 215–220
37. Maletínská, L., Tichá, A., Nagelová, V., Spolcová, A., Blechová, M., Elbert, T., and Zelezná, B. (2013) Neuropeptide FF analog RF9 is not an antagonist of NPFF receptor and decreases food intake in mice after its central and peripheral administration. *Brain Res.* **1498,** 33–40
38. Sun, Y. L., Zhang, X. Y., He, N., Sun, T., Zhuang, Y., Fang, Q., Wang, K. R., and Wang, R. (2012) Neuropeptide FF activates ERK and NF kappa B signal pathways in differentiated SH-SY5Y cells. *Peptides* **38,** 110–117
39. DeWire, S. M., Ahn, S., Lefkowitz, R. J., and Shenoy, S. K. (2007) β-Arrestins and cell signaling. *Annu. Rev. Physiol.* **69,** 483–510
40. Asai, D., Toita, R., Murata, M., Katayama, Y., Nakashima, H., and Kang, J. H. (2014) Peptide substrates for G protein-coupled receptor kinase 2. *FEBS Lett.* **588,** 2129–2132
41. Pronin, A. N., and Benovic, J. L. (1997) Regulation of the G protein-coupled receptor kinase GRK5 by protein kinase C. *J. Biol. Chem.* **272,** 3806–3812
42. Singh, V., Raghuwanshi, S. K., Smith, N., Rivers, E. J., and Richardson, R. M. (2014) G protein-coupled receptor kinase-6 interacts with activator of G protein signaling-3 to regulate CXCR2-mediated cellular functions. *J. Immunol.* **192,** 2186–2194
43. Daaka, Y., Pitcher, J. A., Richardson, M., Stoffel, R. H., Robishaw, J. D., and Lefkowitz, R. J. (1997) Receptor and G$\beta\gamma$ isoform-specific interactions with G protein-coupled receptor kinases. *Proc. Natl. Acad. Sci. U.S.A.* **94,** 2180–2185
44. Celver, J., Xu, M., Jin, W., Lowe, J., and Chavkin, C. (2004) Distinct domains of the mu-opioid receptor control uncoupling and internalization. *Mol. Pharmacol.* **65,** 528–537
45. Jin, W., Brown, S., Roche, J. P., Hsieh, C., Celver, J. P., Kovoor, A., Chavkin, C., and Mackie, K. (1999) Distinct domains of the CB1 cannabinoid receptor mediate desensitization and internalization. *J. Neurosci.* **19,** 3773–3780
46. Gärtner, F., Seidel, T., Schulz, U., Gummert, J., and Milting, H. (2013) Desensitization and internalization of endothelin receptor A: impact of G protein-coupled receptor kinase 2 (GRK2)-mediated phosphorylation. *J. Biol. Chem.* **288,** 32138–32148
47. Ouedraogo, M., Lecat, S., Rochdi, M. D., Hachet-Haas, M., Matthes, H., Gicquiaux, H., Verrier, S., Gaire, M., Glasser, N., Mély, Y., Takeda, K., Bouvier, M., Galzi, J. L., and Bucher, B. (2008) Distinct motifs of neuropeptide Y receptors differentially regulate trafficking and desensitization. *Traffic* **9,** 305–324
48. Butcher, A. J., Hudson, B. D., Shimpukade, B., Alvarez-Curto, E., Prihandoko, R., Ulven, T., Milligan, G., and Tobin, A. B. (2014) Concomitant action of structural elements and receptor phosphorylation determines arrestin-3 interaction with the free fatty acid receptor FFA4. *J. Biol. Chem.* **289,** 18451–18465
49. Williams, J. T., Ingram, S. L., Henderson, G., Chavkin, C., von Zastrow, M., Schulz, S., Koch, T., Evans, C. J., and Christie, M. J. (2013) Regulation of mu-opioid receptors: desensitization, phosphorylation, internalization, and tolerance. *Pharmacol. Rev.* **65,** 223–254
50. Shukla, A. K., Manglik, A., Kruse, A. C., Xiao, K., Reis, R. I., Tseng, W. C., Staus, D. P., Hilger, D., Uysal, S., Huang, L. Y., Paduch, M., Tripathi-Shukla, P., Koide, A., Koide, S., Weis, W. I., Kossiakoff, A. A., Kobilka, B. K., and Lefkowitz, R. J. (2013) Structure of active β-arrestin-1 bound to a G-protein-coupled receptor phosphopeptide. *Nature* **497,** 137–141